

Burn severity and vegetation type control phosphorus concentration, molecular composition, and mobilization

Morgan E. Barnes¹, J. Alan Roebuck, Jr.², Samantha Grieger², Paul J. Aronstein³, Vanessa A. Garayburu-Caruso¹, Kathleen Munson², Robert P. Young¹, Kevin D. Bladon⁴, John D. Bailey⁴, Emily B. Graham^{1,5}, Lupita Renteria¹, Peggy A. O'Day³, Timothy D. Scheibe¹, Allison N. Myers-Pigg^{2,6}

¹ Pacific Northwest National Laboratory, Richland, WA, USA

² Pacific Northwest National Laboratory, Sequim, WA, USA

³ Environmental Systems, University of California - Merced, Merced, CA, USA

⁴ College of Forestry, Oregon State University, Corvallis, OR, USA

⁵ School of Biological Sciences, Washington State University, Pullman, WA, USA

⁶ Department of Environmental Sciences, University of Toledo, Toledo, OH, USA

Correspondence to:

Allison Myers-Pigg (allison.myers-pigg@pnnl.gov)

Morgan Barnes (morgan.barnes@pnnl.gov)

Present Addresses:

Robert P. Young – Washington River Protection Solutions, P.O. Box 850 MSIN M0-01, Richland, WA 99354

Keywords: char; fire impact; ³¹P NMR; P XANES; sagebrush shrubland; Douglas-fir forest; organic matter; nutrient release

Abstract

Shifting phosphorus (P) dynamics after wildfires can have cascading impacts from terrestrial to aquatic environments. However, it is unclear if shifts in P composition or P concentration are responsible for changes in P dynamics post-fire. We used laboratory leaching experiments of Douglas-fir forest and sagebrush shrubland chars to examine how the potential mobility of P compounds is influenced by different burn severities. Burning produced a 6.9- and 29- fold increase in particulate P mobilization, but a 3.8- and 30.5- fold decrease in aqueous P released for Douglas-fir forest and sagebrush shrubland, respectively. The mechanisms driving particulate and dissolved phase P compound mobilization were contrasting. Phosphorus compound mobilization in the particulate phase was controlled by solid char total P concentrations while the aqueous phase was driven by solubility changes of molecular species. Nuclear magnetic resonance and X-ray absorption near edge structure on the solid chars indicated that organic orthophosphate monoester and diester species were thermally mineralized to inorganic P moieties with burning in both vegetation types, which decreases P solubility. This coincided with the production of calcium- and magnesium-bound inorganic P compounds. With increasing burn severity there were systematic shifts in P concentration and composition— higher severity chars mobilized P compounds in the particulate phase, although the magnitude of change was vegetation specific. Our results indicate a post-fire transformation to both the composition of the solid charred material and to how P compounds are mobilized, which may influence its environmental cycling and fate.

Short Summary

Wildfires impact nutrient cycles on land and in water. We used burning experiments to understand the types of phosphorous (P), an essential nutrient, that might be released to the environment after different types of fires. We found the amount of P moving through the environment post-fire is dependent on the type of vegetation and degree of burning which may influence when and where this material is processed or stored.

1 Introduction

Wildfires are a major modifier of the terrestrial landscape, directly burning around 4% of the Earth's surface each year (Randerson et al., 2012). They affect both the terrestrial and adjacent aquatic environments and, as such, are considered one of the largest drivers of aquatic impairment (Ball et al., 2021). The movement of wildfire-derived material from terrestrial landscapes to rivers has impacted 11% of total western United States river length in recent years (Ball et al., 2021). Organic and inorganic nutrient pools and fluxes can be altered by burning through multiple mechanisms. These include the loss of volatile compounds, altered physiochemical properties from the incomplete combustion of organic material (from partially charred biomass to ash; collectively referred to as chars (Bird et al., 2015), and enhanced material transport from leaching and erosion (Bodí et al., 2014). The degree to which wildfires impact ecosystems, or burn severity, is determined by the extent of organic matter loss or change after fire and is influenced by fire intensity, heating duration, degree of live or dead plant material, and fuel moisture, among other factors (Keeley, 2009). Fire frequency, intensity, severity, and total area burned are expected to increase in many regions, such as the western United States (Doerr and Santín, 2016; Haugo et al., 2019; Jolly et al., 2015). In particular, in the Pacific Northwest, USA, burn severity and total burn area have increased in recent decades (Francis et al., 2023; Halofsky et al., 2020; Reilly et al., 2017; Roebuck et al., 2024). Therefore, it is important to understand the mechanisms behind how wildfires alter nutrient quantity, composition, and mobilization.

Phosphorus (P; occurring primarily as orthophosphate H_2PO_4^- , HPO_4^{2-} , or PO_4^{3-}) is an essential element (Smil, 2000) and is often a limiting nutrient to productivity in terrestrial and aquatic environments (Elser et al., 2007). Ecosystem responses post-fire can include shifting terrestrial nutrient acquisition by decreasing phosphatase activity and promoting net primary production (Dijkstra and Adams, 2015; Saa et al., 1993; Vega et al., 2013). Phosphorus-containing compounds transported to aquatic environments can also increase aquatic productivity, influencing invertebrate and fish size and growth rate (Silins et al., 2014). While there is largely an agreement across studies that P becomes enriched in chars after wildfire (Butler et al., 2018; Elliott et al., 2013; García-Oliva et al., 2018; Schaller et al., 2015), with increased concentrations in mineral soil (Butler et al., 2018) and river systems following wildfire (Lane et al., 2008; Mishra et al., 2021; Rust et al., 2018), we are lacking a systematic understanding on how variable burning conditions mediate the P concentration of charred organic material, and the role of different fire-prone vegetation types (but see (Schaller et al., 2015; Wu et al., 2023b; Yusiarni and Gilkes, 2012)) on availability for mobilization. Prescribed burns and wildfires

occur across a range of burning conditions (Merino et al., 2019; Santín et al., 2018; Vega et al., 2013), which results in a mosaic of post-fire ecosystem responses on the landscape (Keeley, 2009). Therefore, understanding how P biogeochemistry is altered along a burn gradient will provide insights on heterogenous responses observed across burned landscapes.

In the environment, P is found in multiple molecular moieties (i.e., orthophosphate, phosphonate, orthophosphate monoester, orthophosphate diester, polyphosphate; orthophosphate monoester and orthophosphate diester compound classes, referred to as the ester bonds moving forward) which exist in different chemical states (i.e., adsorbed on surfaces, incorporated into minerals, precipitated with metals). Chemical speciation influences the solubility and mobility of P, which in turn impacts its bioavailability (Li and Brett, 2013; Turner et al., 2003b; Weihrauch and Opp, 2018; Yan et al., 2023). For example, bonding energy, or strength of the bonds, of the chemical species generally increases from organic P to sorbed and mineral bound P species (Weihrauch and Opp, 2018). The fate of these P species is determined by biological, chemical, physical, and environmental factors, which vary in space and time (Condrón et al., 2015; Yan et al., 2023). Thus, the potential influence of wildfire effects on P dynamics and ecosystem productivity cannot be adequately ascertained by only characterizing P concentration. Compared to changes in total P concentration (i.e. the measure of all P compounds), there is less understanding of P molecular composition in charred material and the impact this has on its mobilization (Robinson et al., 2018; Wu et al., 2023a). As such, it is unclear if P biogeochemical responses post-fire are due to changing composition of the charred material (i.e., composition controlled) and/or an artifact of how P compounds are transported (i.e., mobilized from the solid char to then be transported through the environment). Recent research on laboratory-produced plant-derived chars has demonstrated the use of NMR to quantify P moiety (Sun et al., 2018; Uchimiya and Hiradate, 2014; Wu et al., 2023b; Xu et al., 2016; Yu et al., 2023) and XANES to identify chemical state (Robinson et al., 2018; Rose et al., 2019; Wu et al., 2023a; Yu et al., 2023). Taken together, these complementary techniques are useful tools to provide a holistic understanding of P molecular composition and can help to determine the environmental fate, as certain compounds are preferentially volatilized, produced, and transported across the landscape (Son et al., 2015).

Vegetation burn severity, a common metric to describe how wildfires impact ecosystems, allows for a post-fire assessment of ecosystem impacts (Keeley, 2009). However, relatively few studies relate burn severity to fire effects on P biogeochemistry (Souza-Alonso et al., 2024; Vega et al., 2013) even though it is a more commonly used field metric than fire intensity because it can be measured after the burn (Zavala et al., 2014). Thus, burn severity allows for understanding how burning conditions beyond temperature influence ecosystems. Experimental studies along burn severity gradients provide an opportunity to better understand field conditions post-fire. To understand the amount and types of materials derived from plant litter that could be transported from terrestrial to aquatic systems along a burned gradient, we examined how P concentration and molecular composition in solid chars and their leachates vary across a burn severity gradient. We hypothesize that changing P composition in the solid charred materials with increasing burn severity will influence the leachability of P compounds in the particulate and aqueous phases, and this will be moderated by vegetation type. To test this hypothesis and better understand the amount and types of materials that could be mobilized along a burned gradient, we examined how burn severity influences P concentration and molecular composition in experimentally generated solid chars and their leachates from two common vegetation types present in the Pacific Northwest.

2 Materials and Methods

All datasets and detailed methodology used in this manuscript are available from Grieger et al. (Grieger et al., 2022) version 3 and Barnes et al. (Barnes et al., 2024) on the Environmental System Science Data Infrastructure for a Virtual Ecosystem (ESS-DIVE) repository.

2.1 Burn Experiments

Vegetation was collected from two fire-prone landscapes of contrasting vegetation types to represent archetypes of vegetation commonly found in the Pacific Northwest, USA that also have differing wildfire characteristics (Halofsky et al., 2020; Reilly et al., 2017; Roebuck et al., 2024; Stavi, 2019). In this study, we chose to explore vegetation that is representative of Douglas-fir forests (*Pseudotsuga menziesii*), which tend to burn in the environment at higher intensities, and sagebrush shrublands (*Artemisia tridentata*), which tend to burn at lower intensities (Stavi, 2019). Samples were chosen to be representative of possible living vegetation and litter materials of the dominant species from these landscapes (Grieger et al., 2022; Myers-Pigg et al., 2024; Roebuck et al., 2024). Exact site locations and sampling details can be found in our accompanying data package (Grieger et al., 2022). For Douglas-fir, a mix of living and dead material was collected, while sagebrush was in partial senescence upon collection. All plant materials were air dried for at least two weeks before burning. Woody and canopy materials were mixed at a known ratio (40% materials < 0.5 cm and 60% materials > 0.5 cm) before each burn, and this was held constant for each burn (Grieger et al., 2022).

Chars were generated using an open air burn table, as biochars produced in laboratories have been found to be compositionally different than chars generated in open air burns and wildfires (Myers-Pigg et al., 2024; Santín et al., 2017). To create burns that would result in a range of vegetation burn severities, we manipulated fire behavior on the burn tables by varying burn temperature, duration of heating, fuel moisture content (by experimentally adding moisture to dried materials), fuel density, and vegetation status (i.e., living or litter). Thermocouples were used to monitor temperature over the burn duration, and char grab samples were targeted for 300 °C, 600 °C, and when flames and smoldering commenced (sagebrush shrubland burns did not reach 600 °C). Char burn severity was classified following US Forest Service field metrics based on ash color, degree of consumption, and degree of char (Grieger et al., 2022; Parsons et al., 2010) (Fig. S1). Thus, burn severity was determined by the extent of organic matter loss or change after fire and is influenced by fire intensity, heating duration, degree of live or dead plant material, and fuel moisture, among other factors (Keeley, 2009). Unburned samples and chars were air dried; subsamples were finely ground for elemental composition and were stored in the dark at room temperature until further analysis.

2.2 Elemental Analysis of Solid Samples

Total P, sulfur (S), aluminum (Al), iron (Fe), magnesium (Mg), calcium (Ca), sodium (Na), and potassium (K) were measured using an inductively coupled plasma optical emission spectrometer (ICP-OES) model Optima 7300 DV (PerkinElmer, Waltham, MA). Solid samples were digested with aqua regia at 130 °C for 8 h in an incubation oven (ThermoFisher Scientific, Waltham, MA).

For samples that underwent NMR analysis, approximately 0.5 g of finely ground sample was extracted in a 10 mL solution of 0.25 M NaOH and 0.05 M EDTA for 16 h, followed by

centrifugation, filtration, and measurement on ICP-OES (Sun et al., 2018; Turner et al., 2003b). The goal of the NaOH-EDTA extraction is to get the maximum amount of P into solution. Extraction efficiencies are reported in Table S1 (see SI section Method Limitations for additional information).

2.3 Solution ^{31}P NMR on Solid Samples

After aliquoting 3 mL of the NaOH-EDTA extracts for ICP-OES, the remaining supernatants were frozen and lyophilized to concentrate the extracted compounds. Immediately prior to running NMR experiments (Environmental Molecular Science Laboratory; EMSL, Richland, WA), freeze-dried extracts were reconstituted in 0.52 mL deuterium oxide (D_2O) and 0.26 mL of 10 M NaOH, and 0.52 mL of a solution containing 0.5 M NaOH and 0.1 M EDTA. Full experimental ^{31}P NMR measurement details are provided in the supporting information. In brief, NMR measurements were conducted on an Agilent DD2 spectrometer operating at a field strength of 14.1T (242.95 MHz ^{31}P), equipped with a 5mm Varian broadband direct detect probe. Experiments were conducted at a regulated temperature of 20.0°C. A standard 1D pulse and acquire experiment was performed using a 90° pulse width and recycle delay equal to $5 \times T_1$, which were calibrated and measured individually for each sample using the orthophosphate peak present in each. Samples were measured for 16 h each with the number of transients acquired dependent upon T_1 for each individual sample. Post-acquisition processing and analysis was performed using Mnova 14.0.1 (Mestrelab Research, Spain). Details regarding classification of major P forms, identification of specific P compounds from spiking experiments, quantitation, and method limitations are described in detail in the supporting information (Cade-Menun, 2015; Doolette et al., 2009; Recena et al., 2018) (Fig. S2).

2.4 Solid Sample P XANES

X-ray absorption near edge structure (XANES) is a complementary technique to solution ^{31}P NMR because it can discern the complexation environment of P in solid samples (see SI section Method Limitations for additional information). Bulk XANES was conducted on beamline 14-3 at the Stanford Synchrotron Radiation Lightsource (SSRL, Stanford, CA). The beamline was calibrated at the P K-edge with the first peak of tetraphenylphosphonium bromide at 2146.96 eV.

Sample spectra were fit using least-squares linear combination in Athena (Ravel and Newville, 2005) (Fig. S3). Baseline correction and edge-step normalization parameters were varied for individual samples and reference compounds to reduce error (Werner and Prietzel, 2015). Fits were performed with the component sum not forced to unity, a maximum of three reference compounds, and only fits within $\pm 2.5\%$ were used. If a component fit $< 5\%$, then this reference compound was removed, and the sample was refit with the remaining compounds. The R-factor of all sample fits were < 0.05 (Table S2), indicating a good quality of fit (Kelly et al., 2015). Fits were performed with a variety of Ca, Al, Fe, Mn, K, and Na inorganic and organic P-containing reference compounds. Individual inorganic P compounds (P_i ; includes phosphate and pyrophosphate moieties) reference compounds were grouped based on the associated metal and all organic P compounds (P_o ; includes monoester and diester moieties) were kept as a separate category (Fig. S3; Table S3). Additional information on sample preparation, linear combination fits, reference compounds, and method limitations are described in the supplemental information (XANES Methodology section).

2.5 Leaching Experiments

Leachates from unburned material and char samples were generated in triplicate. Briefly, 25 g of unground sample was shaken in the dark for 24 h in 1000 mL of synthetic rainwater (pH ~ 5) to simulate what might be mobilized by rain events from the solid material and subsequently transported from terrestrial to aquatic environments (Grieger et al., 2022). Our starting mass was kept constant to understand differences in the amounts of materials leached across burn severity gradients, and so our results are directly comparable to temperature gradient studies (Bostick et al., 2018). Therefore, leaching experiments had a different goal of simulating natural mobilization of P compared to the NMR extractions, where we tried to maximize P extracted. Leachates were filtered through a PTFE mesh (2 mm x 0.6 mm) followed by a pre-combusted GF/F filter (< 0.7 µm). Aliquots were immediately taken for subsequent analysis and preserved according to analytical needs described below.

2.6 Elemental Analysis of Leachates

Coarse filtered (< 2 mm) and < 0.7 µm filtered (i.e., aqueous phase) leachates were preserved in 1% nitric acid and stored at 4 °C until analysis. Aliquots of 5 mL were transferred to 15 mL centrifuge tubes, acidified to 10% (v/v) trace metal grade hydrochloric acid and 4% (v/v) trace metal grade nitric acid. Tubes were fully sealed and heated at 85 °C for 2.5 h in an incubation oven (ThermoFisher Scientific, Waltham, MA) and then total elemental analysis were measured by ICP-OES. Total P of the leachate particulate phase (2 mm to 0.7 µm) was calculated as the difference between the coarse filtered and aqueous phase.

Molybdate reactive P was determined on aqueous phase leachate aliquots preserved in 0.2% sulfuric acid and stored at 20 °C, following EPA method 365.3 (Method 365.3: Phosphorus, All Forms (Colorimetric, Ascorbic Acid, Two Reagent)). Aqueous non-molybdate reactive P was calculated as the difference between aqueous total P (as measured by ICP-OES) and molybdate reactive P.

2.7 Data Analyses

Leachable P (mg g P⁻¹; particulate and aqueous phases separately) was calculated by normalizing to the P concentration of the solid samples following Equation 1 (Fischer et al., 2023):

$$\text{Leachable } P_{\text{particulate or aqueous}} = \frac{\text{leachate } P \text{ (mg L}^{-1}\text{)} \times \text{leaching volume (L)}}{\text{mass of dry char (g)} \times \text{P content of dry char (mg P g}^{-1}\text{)}}$$

All statistical tests were conducted in R version 4.2.3 (R Core Team, 2023). Data calculations, statistical analyses, and figures are freely available (Barnes et al., 2024). For all statistical analyses, model assumptions were assessed with a Shapiro-Wilk test of normality using the package stats (R Core Team, 2023) and spread-location plots to inspect homoscedasticity. All analyses met assumptions after log transformation. Significance was determined at the $\alpha = 0.05$ level. All data are reported as the mean \pm standard deviation unless otherwise stated.

Separate analysis of variance (ANOVA) models were used to test how burn severity, vegetation type, and their interaction influences solid P concentration. For leachate samples (i.e., particulate total P, aqueous total P, aqueous molybdate reactive P), mixed-effect models were run with the same fixed effects as the solid samples and a random effect was used to account for triplicate leachates produced from the same solid sample. Mixed effect models were performed with the

lme4 package (Bates et al., 2015) and were fit by maximum likelihood. Variance Inflation Factors were used to inspect for multi-collinearity of fixed effects with the car package (Fox and Weisberg, 2018). Post-hoc pairwise comparisons were conducted using least squares means in the emmeans package (Lenth, 2023). These data are presented in boxplots, which denote the first and third quartiles as the lower and upper hinges, while the whiskers are the largest and smallest values up to 1.5 times the interquartile range. Outliers are captured as individual points on the boxplots, as they are outside the whiskers.

Path analysis was conducted to analyze the hypothesized relationships that may explain how burn severity and vegetation type influence P compound mobilization (i.e., leachable particulate or aqueous phase P concentration) indirectly through changes in char conditions (i.e., P concentration and chemical composition). Calcium-bound P_i was used as a proxy for chemical composition because it is a primary control of P compound solubility in charred materials (Schaller et al., 2015; Uchimiya and Hiradate, 2014; Wu et al., 2023b; Yu et al., 2023). Phosphorus compound mobilization was estimated as the average leachable P from the parent solid samples. Models were run with the sem package (Fox, 2006), with burn severity and vegetation type directly impacting the P concentration and proportion of Ca- P_i in the solid samples, which in turn influence the leachable P concentration. Vegetation type is also set up to directly impact burn severity (Fig. S4).

3 Results and Discussion

3.1 The magnitude of char P increase with burn severity depends on vegetation type

In our study, using experimental open air burns, we found total P concentration (measured using ICP-OES) increased with burn severity in both Douglas-fir forest and sagebrush shrubland solid samples (Fig. 1). Our findings were consistent with observations of increasing P concentration from laboratory-produced chars (García-Oliva et al., 2018; Zheng et al., 2013) and in chars collected shortly after wildfire and prescribed burns (Butler et al., 2018). In particular, while our burn treatments did not reach temperatures that would result in P volatilization, they did represent heterogeneous burn conditions, incorporating a variety of burn durations and temperature ranges (Grieger et al., 2022; Myers-Pigg et al., 2024) that are consistent with other open air burn experiments (Brucker et al., 2022, 2024) (Table 1; Fig. S1). The P concentration in unburned Douglas-fir forest samples was 1.3 ± 0.5 g P kg⁻¹ and increased to an average of 6.2 ± 1.9 g P kg⁻¹ in high-severity burns (ANOVA post hoc $p < 0.001$). On the other hand, unburned sagebrush shrubland material contained 1.3 g P kg⁻¹ compared to 14.5 ± 3.5 g P kg⁻¹ in the moderate-severity burns (ANOVA post hoc $p < 0.001$), the highest severity classes reached for each vegetation type. The observed increase in char P indicated that retention (i.e., condensation) outweighed loss via volatilization. Generally, P and metal cations volatilize at higher temperatures (>774 °C or greater) than carbon (C) and nitrogen (N) (>200 °C), so they are often retained in charred material rather than lost in gaseous form (Son et al., 2015).

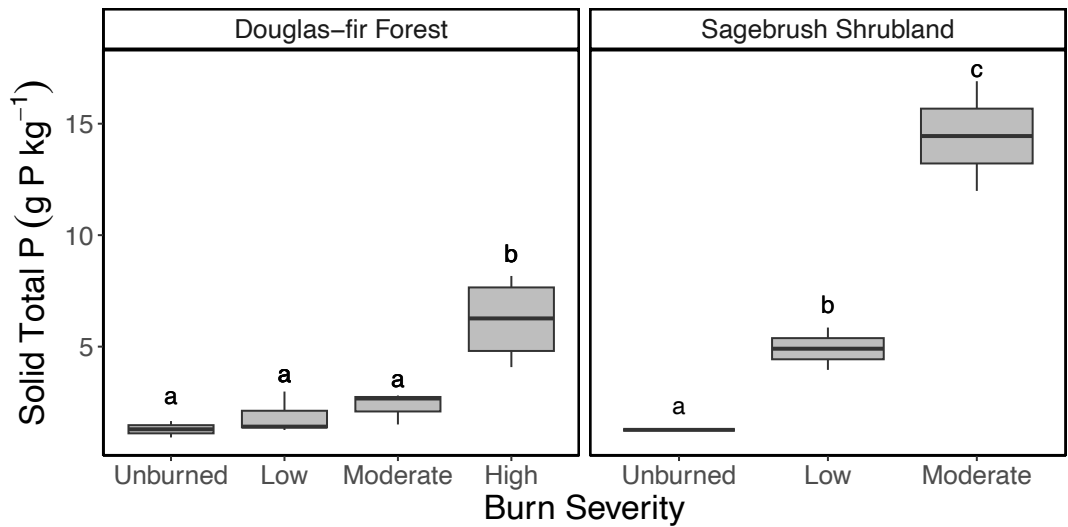


Figure 1. Boxplot of P concentration (g P kg^{-1}) in the solid samples along Douglas-fir Forest and Sagebrush shrubland burn severity gradients. Letters denote post hoc findings of burn severity significant differences within a vegetation type, where the same lettering indicates no significant difference. See Table 1 for burn duration, temperature, and sample size.

300 Although P concentration in solid samples increased from unburned to the highest severity
301 classification reached in both vegetation types, the magnitude was vegetation dependent
302 (ANOVA interaction term: $F = 6.23$, $p = 0.014$). In Douglas-fir forest chars, P concentration was
303 unchanged by burning until high-severity was reached (post hoc test; low: $p = 0.658$, moderate: p
304 $= 0.277$, high: $p < 0.001$), while P in sagebrush shrubland chars increased even after low-severity
305 burns (post hoc test; low: $p = 0.034$, moderate: $p < 0.001$). Post hoc tests further identified that
306 the P concentration of sagebrush shrubland chars was significantly greater than Douglas-fir
307 forest within the same burn severity classification (low: $p = 0.0038$; moderate: $p < 0.001$), even
308 though unburned samples were not statistically different ($p = 0.962$). On average, total P in
309 sagebrush shrubland chars were 2.7 and 6.2 times higher than Douglas-fir forest in low and
310 moderate-severity burns, respectively (Fig. 1).

311 Remarkably, P in moderate-severity sagebrush shrubland chars was even higher than Douglas-fir
312 forest high-severity chars; these represent the highest burn severity observed for each vegetation
313 type. Higher maximum char temperatures or burn duration does not explain why P concentration
314 is greater in burned sagebrush shrubland material compared to Douglas-fir forest; sagebrush
315 shrublands experienced lower temperatures (530 ± 25 °C) and burn duration (202 ± 3 minutes) in
316 moderate-severity burns compared to Douglas-fir forest high-severity burns (704 ± 78 °C; $783 \pm$
317 195 minutes; Table 1).

318
319
320

Burn Severity	Vegetation	Burn Duration (Minutes)	Lowest Max Temp (°C)	Highest Max Temp (°C)	n solids	n leachates
Unburned	Douglas-fir forest	NA	25	25	2	6
	Sagebrush shrubland	NA	25	25	1	3
Low	Douglas-fir forest	342 (403)	295	627	5	15
	Sagebrush shrubland	131 (104)	308	512	2	6
Moderate	Douglas-fir forest	456 (303)	589	757	3	9
	Sagebrush shrubland	202 (3)	512	547	2	6
High	Douglas-fir forest	783 (195)	589	757	4	12

Table 1. Burn characteristics for severity classifications for each vegetation type including mean (standard deviation) duration, mean (standard deviation) maximum temperature reached, low and high range of maximum temperature, and count of the solid and leachate samples.

One mechanism that could explain such results is that sagebrush shrublands may be composed of volatile organic compounds that are more susceptible to loss compared to Douglas-fir forests, leading to selective enrichment of P compounds relative to Douglas-fir forest chars. However, emission factors and total volatile organic compounds from sagebrush and coniferous fuels are relatively similar (Hatch et al., 2019; McMeeking et al., 2009). This suggests that the observed enrichment of sagebrush shrubland P with burning may be due to differences in the conversion of organic P to inorganic P in the sagebrush shrubland materials, which can arise from different fire conditions (Fiddler et al., 2024). Sagebrush shrublands may be more susceptible to changing P dynamics post-fire because chars are likely enriched in P to a greater extent than Douglas-fir forests, even at low severities.

3.2 Solid char molecular composition is influenced by burn severity and vegetation type

Organic P in the solid char was progressively transformed to inorganic species across both vegetation types. Unburned Douglas-fir forest and sagebrush shrubland had similar initial percentages of total organic P with $40.5 \pm 3.3\%$ and 53.7% , respectively (identified by NMR extracts, Fig. 2; also supported by XANES on solid phase, Fig. 3). As burning progressed, the total organic P pools reduced to only $12.6 \pm 8.2\%$ for Douglas-fir forest and $10.4 \pm 8.4\%$ for sagebrush shrubland low-severity chars. While organic P moieties were still present in Douglas-fir forest chars produced at moderate severities ($4.4 \pm 4.2\%$), $<1\%$ was measured in sagebrush shrubland. Moderate-severity sagebrush shrubland chars more closely resembled high-severity Douglas-fir forest with nearly all organic P moieties lost ($<1\%$). This further supports the conclusion that different fire conditions were experienced by Douglas-fir forest and sagebrush shrubland in our simulated burns. Although it has been suggested that organic P can be fully transformed to inorganic species at $200\text{ }^{\circ}\text{C}$ (García-Oliva et al., 2018), another study of organic horizons found organic P moieties persisted after low, moderate, and high-severity fires that reached up to $872\text{ }^{\circ}\text{C}$ (Merino et al., 2019). We measured organic P in burns that reached above $600\text{ }^{\circ}\text{C}$, suggesting that the thermal mineralization of organic to inorganic P compounds is

controlled by microscale differences in temperature and selective physical protection (i.e., mineral aggregates) rather than what is observed at overall bulk temperatures, and is likely a result of the interaction between temperature, burn duration, and vegetation type experienced by these microsites (Galang et al., 2010; Lopez et al., 2024).

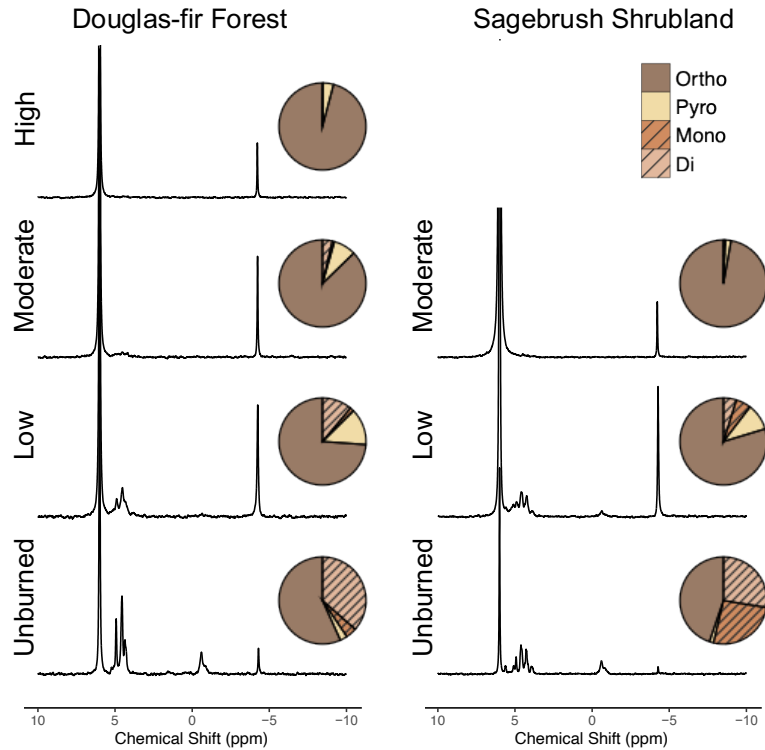


Figure 2. Solution ^{31}P nuclear magnetic resonance (NMR) spectra from a representative solid char sample of each burn severity and vegetation type. The number of scans varied for each sample, based on relaxation time, and therefore direct comparisons of peak intensities can only be made within a spectrum (see additional details in SI NMR Methods). Averaged replicates are represented by pie charts for the proportions of orthophosphate (ortho), pyrophosphate (pyro) monoesters (mono) and diesters (di). Orthophosphate and pyrophosphate are inorganic species (brown colors) and monoester and diesters are organic species (orange colors with hashed lines). Ranges of maximum temperatures ($^{\circ}\text{C}$) reached within a respective burn severity category are reported in parentheses. See SI sections NMR Methodology and Method Limitations for additional details and Table 1 for burn duration, temperature, and sample size.

Previous studies have suggested charred materials containing diester species (two C moieties per P) are more vulnerable to thermal mineralization than monoesters (one C moiety per P) (García-Oliva et al., 2018; Turrion et al., 2010). However, we found diester and monoester species followed similar proportional decreases in our chars with burning (Fig. S5). Hence, both readily available (i.e., diester) and less labile (i.e., monoester) organic P species (Condon et al., 2015) were converted to inorganic P at comparable rates, which is similar to forest and shrubland organic horizons subjected to prescribed fire (Merino et al., 2019). This suggests there is not a fundamental molecular difference in how these moieties respond to burning in organic material

such as what is examined in our study, but instead the preferential loss of diesters in burned mineral soil may be because the stronger sorption of monoesters to soil particles attenuates the heat.

Because diester and monoester species were lost at similar proportions, the composition of the unburned material dictated the resulting char P composition and potential bioavailability. Across both vegetation types, we identified phospholipids, DNA, and RNA (diester region) and phytate and sugar phosphates (monoester region; Fig. 2; Table S4), which follows other studies of vegetation P composition (Doolette and Smernik, 2016; Noack et al., 2012). However, the proportions of these species were vegetation dependent, where unburned Douglas-fir forest was dominated by diesters ($36.5 \pm 9.1\%$) with minor percentages of monoesters ($4.1 \pm 5.7\%$), whereas sagebrush shrubland was nearly equal parts diesters (27.6%) and monoesters (26.1%). RNA, DNA, phospholipids, and sugar phosphates are considered bioavailable due to their weak adsorption, whereas phytate strongly sorbs to both organic and inorganic particles making it relatively less available for biological uptake (Condrón et al., 2015; Li and Brett, 2013; Turner et al., 2003a). Douglas-fir forest was composed of a greater proportion of these bioavailable organic species in unburned ($36.8 \pm 7.6\%$) and low-severity burns ($12.4 \pm 8.4\%$) compared to sagebrush shrubland (unburned: 32.4; low: $8.0 \pm 4.5\%$).

With increased burn severity, Douglas-fir forest (high-severity) and sagebrush shrubland (moderate-severity) organic speciation converged with only $< 1\%$ of organic P (as RNA) remaining. Prior studies using NMR in plant-based biochar produced from 300 – 800 °C found char was composed of entirely inorganic P, including orthophosphate (27–97%) and pyrophosphate (3–71%; although one sample produced at 350 °C was 2% phospholipids) (Sun et al., 2018; Uchimiya et al., 2015; Uchimiya and Hiradate, 2014). The unburned parent material in these studies had variable starting compositions with organic P ranging from 3–87% (as phytate). The extent of organic P loss in these studies is most similar to our higher severity samples, once again demonstrating that more than temperature determines the composition of P in charred material. Overall, these findings suggest organic P moieties in charred material are determined by the degree of burning, where lower severity chars resemble the starting composition, and this is influenced by vegetation type.

As organic species were thermally mineralized in our chars, inorganic P, such as pyrophosphate, was produced (Fig. 2). Pyrophosphate can be produced either from orthophosphate or phytate and is thought to largely originate from fungal tissue (Bünemann et al., 2008; Makarov et al., 2005), although it has been found in some plants (Noack et al., 2012; Wu et al., 2023b). We found pyrophosphate peaked in low-severity chars across both vegetation types, reaching $13.6 \pm 3.1\%$ in Douglas-fir forest and $9.9 \pm 6.2\%$ in sagebrush shrubland burns. Prior NMR studies on plant chars produced between 350 - 800 °C have also observed an increase in the proportion of pyrophosphate relative to unburned material, followed by a decrease at higher charring conditions (Sun et al., 2018; Uchimiya and Hiradate, 2014). Variability in pyrophosphate from naturally produced chars has also been observed. For example, post wildfire, pyrophosphate was ~3% in a pine forest (García-Oliva et al., 2018), absent in a eucalyptus forest (Santín et al., 2018), 0–13% of cedar-hemlock forests (Cade-Menun et al., 2000), and 3–7% from pine forests and shrublands (Merino et al., 2019). Thus burned organic material, especially in chars produced at low-severity wildfire and prescribed burns, may be an important, yet underappreciated, source of pyrophosphate in the environment.

The production of pyrophosphate in our charred plant material is likely a result of the initial organic matter composition and burning conditions (Wu et al., 2023b; Yu et al., 2023). Pyrophosphate and other polyphosphates can be produced from orthophosphate during burning, with the thermal degradation of phytate (organic P; monoester) contributing more orthophosphate (Robinson et al., 2018; Rose et al., 2019; Uchimiya and Hiradate, 2014). Pyrophosphate was greater in Douglas-fir forest chars compared to sagebrush shrublands, even though sagebrush shrubland chars contained more phytate in the unburned material (Fig. 2). This indicates pyrophosphate was primarily produced from polymerization and dehydration of orthophosphate, and not from thermal degradation of phytate in our chars (Uchimiya and Hiradate, 2014).

Although pyrophosphate peaked in low-severity chars, we found the percentage of total inorganic P species continued to increase with burning across both vegetation types, as measured by NMR on solid extracts and XANES of intact solid samples (Fig. 2, Fig. 3; Tables S2 and S4), demonstrating additional transformations to P composition with increasing severity. Inorganic species, measured by XANES, in unburned material was composed largely of P compounds associated with Fe (37% sagebrush shrubland; $40 \pm 5\%$ Douglas-fir forest; fitting primarily as P_i sorbed to the surface of goethite) and a minor component of Ca-bound P_i species ($3 \pm 3\%$ Douglas-fir forest; 9% sagebrush shrubland; fitting mostly as apatite). The proportion of Ca- and Mg- P_i (fitting as magnesium phosphate and/or struvite) increased with burn severity (Fig. 3; Table S2). Douglas-fir forest high-severity chars had $52.8 \pm 8.3\%$ Ca- P_i and $29.0 \pm 9.9\%$ Mg- P_i , while sagebrush shrubland moderate-severity chars contained $45.1 \pm 0.1\%$ Ca- P_i and $53.7 \pm 0.1\%$ Mg- P_i .

Other studies using XANES supports the production of Ca- P_i , along with Fe- or Mg- P_i in plant-based chars and ash (Robinson et al., 2018; Sun et al., 2018; Uchimiya and Hiradate, 2014; Wu et al., 2023a), whereas studies using other techniques (solid-state NMR, sequential fractionation) have found higher temperatures result in greater Ca- and Al- P_i (García-Oliva et al., 2018; Xu et al., 2016). Hydroxyapatite and other stable forms of Ca- P_i minerals are known to be produced by organic matter combustion (Uchimiya and Hiradate, 2014), so it follows that these P species are produced with burning and progressively increase along our burn severity gradient. P compound bonding environments have been found to resemble stoichiometric ratios of the burned material (Wu et al., 2023a; Zwetsloot et al., 2015). Our findings support this where Ca- and Mg- P_i species increased as the proportion of Ca and Mg also increased (Fig. 3; Tables S2, S5, and S6). Phosphorus mobility and bioavailability of P compounds are likely influenced by increased inorganic P proportions because Ca- P_i , especially apatite, is considered to have low water extractability and apparent bioavailability (García-Oliva et al., 2018; Li and Brett, 2013; Zwetsloot et al., 2015).

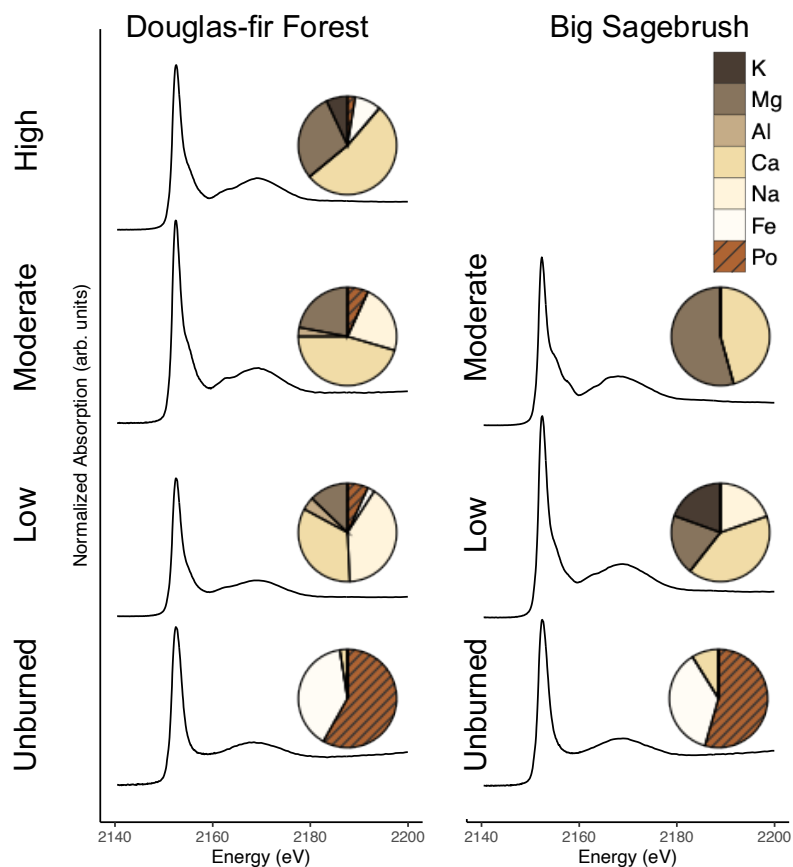


Figure 3. Phosphorus K-edge X-ray absorption near edge structure (XANES) spectroscopy from a representative solid unburned and char sample of each burn severity and vegetation type. Averaged replicates are represented by pie charts for the proportions of P_i associated with K-, Mg-, Al-, Ca-, Na-, and Fe (brown colors) and P_o species grouped together regardless of metal association (orange color with hashed lines; see SI XANES Methods for additional details). Ranges of maximum temperatures ($^{\circ}\text{C}$) reached within a respective burn severity category are reported in parentheses. See SI sections XANES Methodology and Method Limitations for additional details and Table 1 for burn duration, temperature, and sample size.

443

444 3.3 Leachable particulate- and aqueous-bound P have contrasting mobilization patterns with 445 burning and are under differing controls

446 As burn severity increased, the enriched P of the solid chars resulted in greater particulate P
447 mobilized (assessed via leaching experiments), regardless of vegetation type ($\beta = 0.78$, $p <$
448 0.001 , $r^2 = 0.68$; Fig. 4, Fig. 5). Burning resulted in a 6.9- and 29- fold increase of particulate P
449 mobilization from Douglas-fir forest (high-severity) and sagebrush shrubland (moderate-
450 severity) chars, respectively (Fig. 4). Phosphorus compounds may be largely physically protected
451 in the matrix of the charred material (70–90% residual P in sequential fractionation scheme (Wu
452 et al., 2023b)), therefore it follows that particulate P patterns are controlled by changes in solid

char concentration; charred material becomes enriched with P and there is production of highly mobile particulates (such as ash (Blake et al., 2010)). Path analysis identified that burn severity ($\beta = 0.61$, $p < 0.001$) and vegetation type ($\beta = 0.65$, $p < 0.001$) had direct influence on solid char P concentration ($r^2 = 0.64$; Fig. 5). Mixed effect model results further demonstrate that the effect burn severity has on leachable particulate P is vegetation dependent (interaction term of mixed effect model; $p = 0.009$). Moderate-severity sagebrush shrubland chars mobilized 5.2 times more P in the particulate phase than Douglas-fir forest ($p = 0.04$). Particulate P mobilized from charred material can be transported to waterways, as a meta-analysis found unfiltered P concentrations in the western United States increased ~ 1.7 times after wildfire ($n = 46$) (Rust et al., 2018).

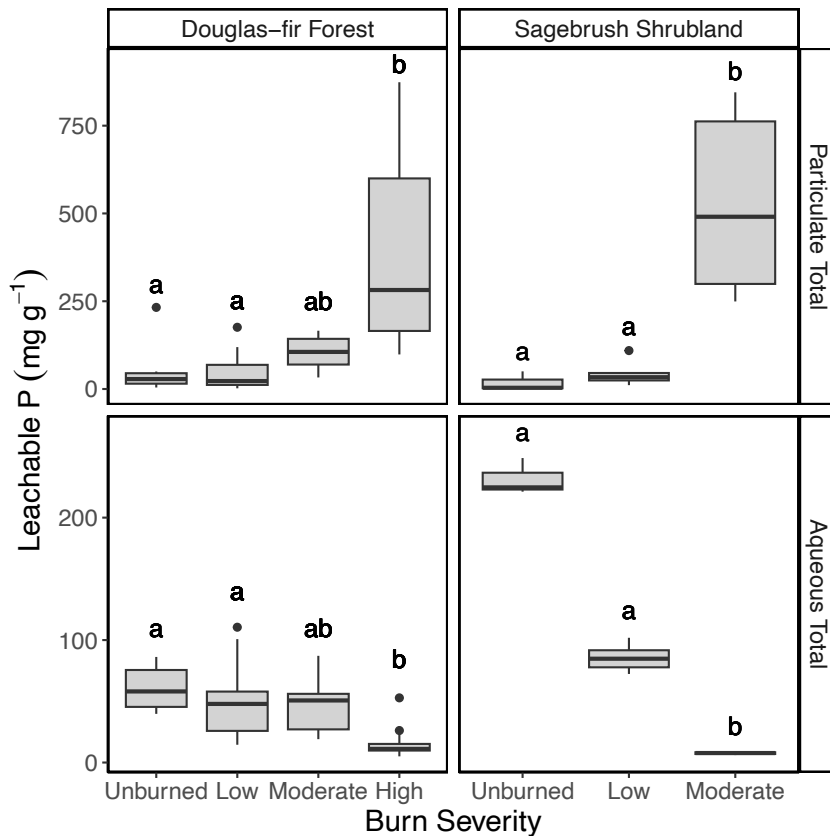


Figure 4. Boxplot of the relationship between burn severity and vegetation type with leachable P concentration (mg P g^{-1} ; calculated from Equation 1) for total P in the particulate phase and total P in the aqueous phase. Molybdate-reactive P in the aqueous phase are reported in the SI. Ranges of maximum temperatures ($^{\circ}\text{C}$) reached within a respective burn severity category are reported in parentheses. Letters denote post hoc findings of burn severity significant differences within a vegetation type, where the same lettering indicates no significant difference. Note difference scales of the y-axis for the particulate and aqueous phases. See Table 1 for burn duration, temperature, and sample size and Figure S6 for leachable aqueous molybdate reactive P results.

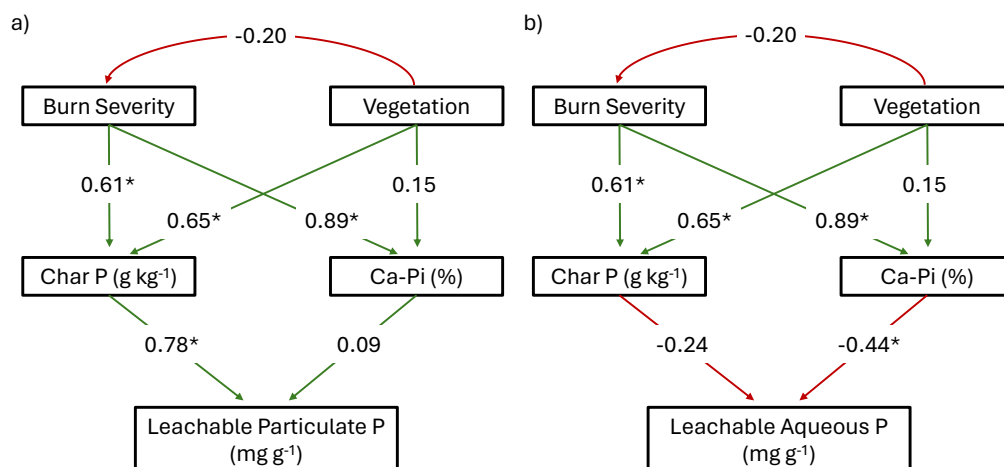


Figure 5. Path analysis model results for the impact of burn severity and vegetation type on leachable P in the (a) particulate and (b) aqueous phases, as mediated by solid unburn and char P concentration and chemical composition. All relationships are reported with significance ($\alpha = 0.05$) denoted with an asterisk symbol on the standardized correlation coefficient (analogous to relative regression weights). Paths are green for positive relationships and red for negative. Leachable Particulate P Model: $\chi^2 = 16.277$, $p < 0.05$, $df = 3$, RMSEA = 0.483, AIC = 108.3; Leachable Aqueous P Model: $\chi^2 = 19.032$, $p < 0.05$, $df = 3$, RMSEA = 0.530, AIC = 122.1. See Fig S4 for original hypothesized model.

In contrast to leachable particulate P, mobilization of P in the aqueous phase decreased 3.8-fold for Douglas-fir forest and 30.5-fold for sagebrush shrubland with burning (Fig. 4). Prior work from laboratory-produced plant chars have found decreased water-soluble P even though solid char concentration increased with burning (Gundale and DeLuca, 2006; Mukherjee and Zimmerman, 2013; Wu et al., 2011; Yu et al., 2023; Zheng et al., 2013). Instead of concentration-controlled like particulate P, aqueous P mobilization was composition-controlled (represented as percentage of Ca-P_i in our path analysis, $\beta = -0.44$, $p = 0.041$, $r^2 = 0.34$; Fig. 5). We chose to represent P composition in the path analysis as Ca-P_i to simplify the path analysis interpretation. In reality, drivers of aqueous P mobilization extend beyond Ca-P_i and include other compositional shifts, such as Mg-P_i, organic P speciation, and pH. Phosphorus compound adsorption to multivalent cations (Ca²⁺, Mg²⁺, Fe³⁺, and Al³⁺) can decrease aqueous phase export (Glaser et al., 2002). Indeed, we found higher severity burns had greater concentrations of metals (Tables S5 and S6) which interacted with P to form primarily Ca- and Mg-P_i species (Fig. 3; Table S2).

Additional changes to char composition, including organic P speciation and pH, also likely contributed to decreased aqueous P mobilization with increased burning. We found a decrease in non-molybdate reactive aqueous P, which is largely composed of organic P species (Condon et al., 2015), with increasing burn severity (mixed effect model interaction term: $p < 0.001$, Fig. S6) indicating less mobilization of organic P species with burning. The amount of mobilized P compounds from char is also related to pH (Fig. 6), where less P compounds are released at higher pH (Silber et al., 2010; Zheng et al., 2013). We found aqueous P mobilization had an inverse relationship with pH for both Douglas-fir forest ($p < 0.001$; $r^2 = 0.45$) and sagebrush shrubland ($p < 0.001$, $r^2 = 0.97$; Fig. 6). Overall, changing chemical composition of the charred

material decreases solubility and therefore reduces aqueous P mobilization into the environment (Robinson et al., 2018; Uchimiya et al., 2015; Wu et al., 2023b; Xu et al., 2016).

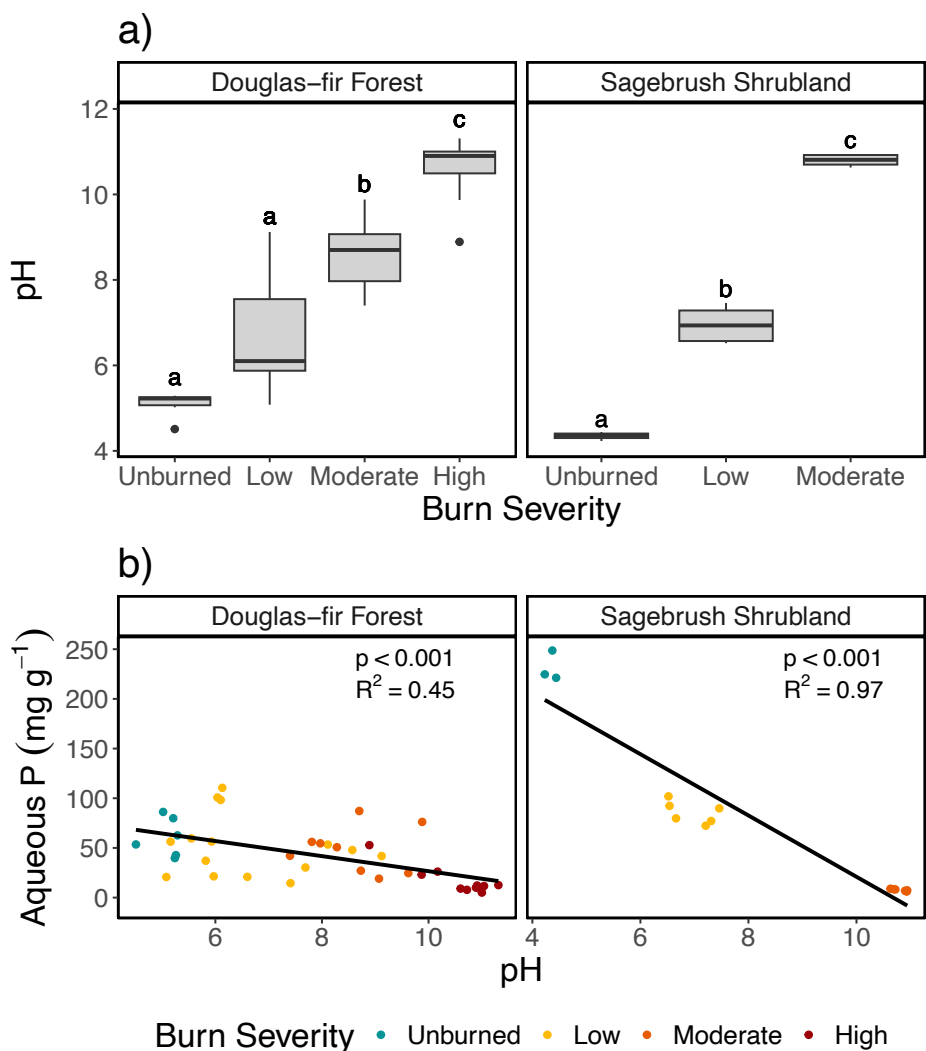


Figure 6. a) Boxplot of pH and burn severity. Letters denote post hoc findings of burn severity significant differences within a vegetation type, where the same lettering indicates no significant difference. See Table 1 for burn duration, temperature, and sample size. B) Relationship between pH and aqueous P for Douglas-fir forest and Sagebrush shrubland.

The extent of decreased aqueous P mobilization was vegetation dependent (interaction term of mixed effect model; $p < 0.001$; Fig. 4). However, because both vegetation types had similar percentages of Ca-P_i ($p = 0.18$; $r^2 = 0.15$), it indicates additional controls on aqueous P mobilization. In addition to Ca-P_i and Mg-P_i, moderate-severity Douglas-fir forest contained P compounds associated with Na (XANES: $22.7 \pm 22.1\%$) and organic P species (XANES: $6.9 \pm 11.9\%$; NMR: $4.4 \pm 4.2\%$), whereas Na-P_i was not detected in sagebrush shrubland and organic P was $<1\%$ (XANES: $0 \pm 0\%$; NMR: $0.7 \pm 0.4\%$; Figs. 2 and 3; Tables S2 and S4). Greater solubility of these chemical species likely contributes to Douglas-fir forest moderate-severity burns mobilizing 6.4 times more aqueous P than sagebrush shrubland ($p = 0.004$). Changing

chemical speciation from soluble organic and inorganic P to less soluble inorganic species (Li and Brett, 2013; Mukherjee and Zimmerman, 2013; Xu et al., 2016) resulted in the decreased export of P compounds with increased burn severity and contributed to the amount of P compounds mobilized from the respective vegetation types. This has important implications for P compounds that are transported in the environment because organic P can leach faster than many inorganic compounds (McDowell et al., 2021) and Na-P_i has been found as having high nutrient uptake and bioavailability (Li and Brett, 2013).

4 Conclusions

We found systematic changes in P chemistry across vegetation types; with increasing burn severity there were systematic shifts in P concentration and composition. We summarize our findings into a conceptual model to synthesize the main findings from this study (Fig. 7). From unburned to high-severity, identifiable structures decreased with increasing black charring and/or white ash (Fig. 7 panel 1; Fig. S1). Total Ca, Fe, Al, K, Ma, and Na concentrations increased (Table S5). Solid char concentration and composition controlled how P compounds were mobilized from burned material. Overall, burning resulted in an increase of char P concentration (Fig. 7 panel 1), which subsequently controlled the mobilization of particulate-bound P compounds from the chars. As burning progressed, chars compositionally transitioned from proportionally more organic P species, including both monoester and diesters, to Ca- and Mg-bound inorganic P species (Fig. 7 panel 1). These compositional changes resulted in less soluble inorganic P species and therefore reduced aqueous P mobilization in higher severity burns (Fig. 7 panel 2). Across vegetation types, chars became more divergent from the unburned vegetation material in P composition and mobilization potential as burning continued. Burn severity and vegetation type indirectly influenced the quantity and leachable phase (i.e., particulate or

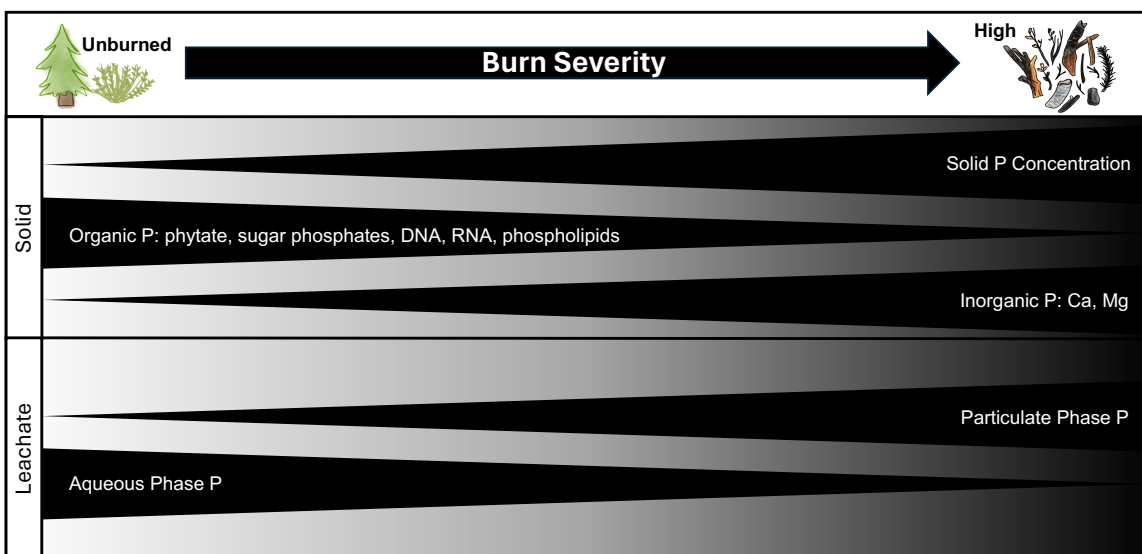


Figure 7. Conceptual framework for phosphorus biogeochemical shifts with increasing burn severity where solid P concentration increases, organic P species decrease while inorganic P increases. Leachates from the solid samples increased in mobilization of P in the particulate phase but decreased in aqueous P with burning.

aqueous) of P compounds that were mobilized from charred material by altering solid sample concentration and composition.

Although both vegetation types followed similar concentration and compositional patterns, sagebrush shrubland had greater P transformations than Douglas-fir forest across our P burn severity conceptual model (Figs. 7 and S4). The P concentration of Douglas-fir forest chars and leachates were more resilient to change with burning compared to sagebrush shrubland. Phosphorus transformations in sagebrush shrubland moderate-severity burns generally chemically resembled that of Douglas-fir forest high-severity burns (i.e., higher solid P concentrations, more particulate leachable P, and more inorganic P). Taken together, this indicates that although sagebrush shrubland experiences more low- and moderate-severity burns than Douglas-fir forests (Stavi, 2019), the response of P chemistry in the environment post-fire may resemble Douglas-fir forests burned at higher severities. This response is important to note as shifts in fire severity are not occurring uniformly across all ecosystem types (Francis et al., 2023; Halofsky et al., 2020; Reilly et al., 2017), which may influence post-fire P dynamics across ecosystems.

The ultimate fate of P in the environment is determined by the interactions among biological, chemical, physical and environmental factors (Condon et al., 2015; Yan et al., 2023). Our leaching experiments provide insight to the potential mobilization mechanisms of P release from solid vegetation chars. The key to bioavailable P is that it can enter solution for subsequent uptake by plants and microbes (Kruse et al., 2015). We found burning resulted in less P released into the environment in the aqueous phase, therefore, the differences in aqueous P we observed with burn severity can influence biogeochemical cycling of P by altering its availability for biological uptake and physical transport. The increase in particulate-bound P may be an important source of available P over longer timeframes, compared to starting vegetation. For instance, P mobilization into riverine systems can be long-lived following fire, altering P budgets and aquatic ecosystem health (Bodí et al., 2014; Emmerton et al., 2020; Rust et al., 2018; Santín et al., 2018; Silins et al., 2014). Our study helps to provide additional information on the potential environmental fate of P post-fire in the context of different burn severities and ecosystem types.

Acknowledgments

We thank Christopher Myers for assistance with the ICP analyses and Sophia McKeever for help with measuring molybdate reactive P. This research was supported by the U.S. Department of Energy, Office of Science, Office of Biological and Environmental Research, Environmental System Science (ESS) Program. This contribution originates from the River Corridor Scientific Focus Area project at Pacific Northwest National Laboratory (PNNL). PNNL is operated by Battelle Memorial Institute for the United States Department of Energy under contract no. DE-AC05-76RL01830. Portions of this research were performed on a project award ([10.46936/lser.proj.2021.51840/60000342](https://www.slac.stanford.edu/programs/ess/focus-areas/river-corridor-scientific-focus-area/)) from the Environmental Molecular Science Laboratory (EMSL) (grid.436923.9), a DOE Office of Science User Facility sponsored by the Biological and Environmental Research program under Contract No. DE-AC05-76RL01830. XANES data were collected from the Stanford Synchrotron Radiation Lightsource, SLAC National Accelerator Laboratory, which is supported by the U.S. Department of Energy, Office of Science, Office of Basic Energy Sciences under Contract No. DE-AC02-76SF00515. We

would like to give a special thanks to Erik Nelson, the beamline scientist from SSRL that helped us collect those data.

Code/Data availability

All data and code are publicly available on the Environmental System Science Data Infrastructure for a Virtual Ecosystem (ESS-DIVE) repository (Barnes et al., 2024; Grieger et al., 2022) .

Competing interests

The authors declare no competing interests.

Author Contribution

Conceptualization: M.E.B., A.N.M.-P., J.A.R., K.D.B., E.B.G., S.G., T.D.S. Methodology and Software: A.N.M.-P., M.E.B., S.G., J.D.B., K.B., E.B.G., P.A., V.A.G-C, K.M, J.A.R., R.P.Y., P.A.O., L.R. Investigation: M.E.B., P.A., S.G., K.M, L.R., J.A.R., J.D.B., K.D.B., R.P.Y. Data Curation: M.E.B., S.G., P.A., V.A.G-C., A.N.M.-P., K.M, J.D.B., K.D.B., L.R., J.A.R. Formal Analysis: M.E.B., A.N.M-P, J.A.R., V.A.G.-C., P.A., P.A.O., R.P.Y. Validation: M.E.B., P.A., K.M., V.A.G.-C., A.N.M-P, P.A.O., R.P.Y. Visualization: M.E.B., A.N.M.-P., S.G. Writing - Original Draft: M.E.B., A.N.M.-P., J.A.R., S.G., K.M., R.P.Y. Writing – Review and Editing: M.E.B., P.A., J.D.B., K.D.B., V.A.G.-C., E.B.G., A.N.M.-P., P.A.O., L.R., J.A.R, T.D.S., R.P.Y.

References

- Ball, G., Regier, P., González-Pinzón, R., Reale, J., and Van Horn, D.: Wildfires increasingly impact western US fluvial networks, *Nat. Commun.*, 12, 2484, 2021.
- Barnes, M. E., Aronstein, P. J., Bailey, J. D., Bladon, K. D., Forbes, B., Garayburu-Caruso, V. A., Grieger, S., Graham, E. B., McKever, S. A., Myers, C. R., Munson, K. M., O’Day, P. A., Powers-McCormack, B., Renteria, L., Roebuck, A., Scheibe, T. D., Young, R. P., and Myers-Pigg, A. N.: Data and scripts associated with: “Burn severity and vegetation type control phosphorus concentration, molecular composition, and mobilization,” <https://doi.org/10.15485/2547035>, 2024.
- Bates, D., Mächler, M., Bolker, B., and Walker, S.: Fitting Linear Mixed-Effects Models Using lme4, *J. Stat. Softw.*, 67, 1–48, 2015.
- Bird, M. I., Wynn, J. G., Saiz, G., Wurster, C. M., and McBeath, A.: The pyrogenic carbon cycle, *Annu. Rev. Earth Planet. Sci.*, 43, 273–298, 2015.
- Blake, W. H., Theocharopoulos, S. P., Skoulikidis, N., Clark, P., Tountas, P., Hartley, R., and Amaxidis, Y.: Wildfire impacts on hillslope sediment and phosphorus yields, *J. Soils Sediments*, 10, 671–682, 2010.

599 Bodí, M. B., Martin, D. A., Balfour, V. N., Santín, C., Doerr, S. H., Pereira, P., Cerdà, A., and
600 Mataix-Solera, J.: Wildland fire ash: Production, composition and eco-hydro-geomorphic effects,
601 Earth-Sci. Rev., 130, 103–127, 2014.

602 Bostick, K. W., Zimmerman, A. R., Wozniak, A. S., Mitra, S., and Hatcher, P. G.: Production
603 and Composition of Pyrogenic Dissolved Organic Matter From a Logical Series of Laboratory-
604 Generated Chars, Frontiers in Earth Science, 6, 43, 2018.

605 Brucker, C. P., Livneh, B., Minear, J. T., and Rosario-Ortiz, F. L.: A review of simulation
606 experiment techniques used to analyze wildfire effects on water quality and supply, Environ. Sci.
607 Process. Impacts, 24, 1110–1132, 2022.

608 Brucker, C. P., Livneh, B., Butler, C. E., and Rosario-Ortiz, F. L.: A laboratory-scale simulation
609 framework for analysing wildfire hydrologic and water quality effects, Int. J. Wildland Fire, 33,
610 <https://doi.org/10.1071/wf23050>, 2024.

611 Bünemann, E. K., Smernik, R. J., Marschner, P., and McNeill, A. M.: Microbial synthesis of
612 organic and condensed forms of phosphorus in acid and calcareous soils, Soil Biol. Biochem.,
613 40, 932–946, 2008.

614 Butler, O. M., Elser, J. J., Lewis, T., Mackey, B., and Chen, C.: The phosphorus-rich signature of
615 fire in the soil-plant system: a global meta-analysis, Ecol. Lett., 21, 335–344, 2018.

616 Cade-Menun, B. J.: Improved peak identification in ³¹P-NMR spectra of environmental samples
617 with a standardized method and peak library, Geoderma, 257–258, 102–114, 2015.

618 Cade-Menun, B. J., Berch, S. M., Preston, C. M., and Lavkulich, L. M.: Phosphorus forms and
619 related soil chemistry of Podzolic soils on northern Vancouver Island. II. The effects of clear-
620 cutting and burning, Can. J. For. Res., 30, 1726–1741, 2000.

621 Condrón, L. M., Turner, B. L., and Cade-Menun, B. J.: Chemistry and dynamics of soil organic
622 phosphorus, in: Phosphorus: Agriculture and the Environment, American Society of Agronomy,
623 Crop Science Society of America, and Soil Science Society of America, Madison, WI, USA, 87–
624 121, 2015.

625 Dijkstra, F. A. and Adams, M. A.: Fire Eases Imbalances of Nitrogen and Phosphorus in Woody
626 Plants, Ecosystems, 18, 769–779, 2015.

627 Doerr, S. H. and Santín, C.: Global trends in wildfire and its impacts: perceptions versus realities
628 in a changing world, Philos. Trans. R. Soc. Lond. B Biol. Sci., 371,
629 <https://doi.org/10.1098/rstb.2015.0345>, 2016.

630 Doolette, A. L. and Smernik, R. J.: Phosphorus speciation of dormant grapevine (*Vitis vinifera* L.)
631 canes in the Barossa Valley, South Australia, Aust. J. Grape Wine Res., 22, 462–468, 2016.

632 Doolette, A. L., Smernik, R. J., and Dougherty, W. J.: Spiking improved solution phosphorus-31
633 nuclear magnetic resonance identification of soil phosphorus compounds, Soil Sci. Soc. Am. J.,
634 73, 919–927, 2009.

635 Elliott, K. J., Knoepp, J. D., Vose, J. M., and Jackson, W. A.: Interacting effects of wildfire
636 severity and liming on nutrient cycling in a southern Appalachian wilderness area, *Plant Soil*,
637 366, 165–183, 2013.

638 Elser, J. J., Bracken, M. E. S., Cleland, E. E., Gruner, D. S., Harpole, W. S., Hillebrand, H.,
639 Ngai, J. T., Seabloom, E. W., Shurin, J. B., and Smith, J. E.: Global analysis of nitrogen and
640 phosphorus limitation of primary producers in freshwater, marine and terrestrial ecosystems,
641 *Ecol. Lett.*, 10, 1135–1142, 2007.

642 Emmerton, C. A., Cooke, C. A., Hustins, S., Silins, U., Emelko, M. B., Lewis, T., Kruk, M. K.,
643 Taube, N., Zhu, D., Jackson, B., Stone, M., Kerr, J. G., and Orwin, J. F.: Severe western
644 Canadian wildfire affects water quality even at large basin scales, *Water Res.*, 183, 116071,
645 2020.

646 Fiddler, M. N., Thompson, C., Pokhrel, R. P., Majluf, F., Canagaratna, M., Fortner, E. C.,
647 Daube, C., Roscioli, J. R., Yacovitch, T. I., Herndon, S. C., and Bililign, S.: Emission factors
648 from wildfires in the Western US: An investigation of burning state, ground versus air, and
649 diurnal dependencies during the FIREX-AQ 2019 campaign, *J. Geophys. Res.*, 129,
650 <https://doi.org/10.1029/2022jd038460>, 2024.

651 Fischer, S. J., Fegle, T. S., Wilkerson, P. J., Rivera, L., Rhoades, C. C., and Rosario-Ortiz, F. L.:
652 Fluorescence and Absorbance Indices for Dissolved Organic Matter from Wildfire Ash and
653 Burned Watersheds, *ACS EST Water*, 3, 2199–2209, 2023.

654 Fox, J.: TEACHER’S CORNER: Structural Equation Modeling With the sem Package in R,
655 *Struct. Equ. Modeling*, 13, 465–486, 2006.

656 Fox, J. and Weisberg, S.: *An R Companion to Applied Regression*, SAGE Publications, 608 pp.,
657 2018.

658 Francis, E. J., Pourmohammadi, P., Steel, Z. L., Collins, B. M., and Hurteau, M. D.: Proportion
659 of forest area burned at high-severity increases with increasing forest cover and connectivity in
660 western US watersheds, *Landsc. Ecol.*, 38, 2501–2518, 2023.

661 Galang, M. A., Markewitz, D., and Morris, L. A.: Soil phosphorus transformations under forest
662 burning and laboratory heat treatments, *Geoderma*, 155, 401–408, 2010.

663 García-Oliva, F., Merino, A., Fonturbel, M. T., Omil, B., Fernández, C., and Vega, J. A.: Severe
664 wildfire hinders renewal of soil P pools by thermal mineralization of organic P in forest soil:
665 Analysis by sequential extraction and ³¹P NMR spectroscopy, *Geoderma*, 309, 32–40, 2018.

666 Glaser, B., Lehmann, J., and Zech, W.: Ameliorating physical and chemical properties of highly
667 weathered soils in the tropics with charcoal – a review, *Biol. Fertil. Soils*, 35, 219–230, 2002.

668 Grieger, S., Bailey, J., Barnes, M., Bladon, K. D., Forbes, B., Garayburu-Caruso, V. A., Graham,
669 E. B., Goldman, A. E., Homolka, K., McKeever, S. A., Myers-Pigg, A., Otenburg, O., Renteria,
670 L., Roebuck, A., Scheibe, T. D., and Torgeson, J. M.: Organic Matter Concentration and
671 Composition of Experimentally Burned Open Air and Muffle Furnace Vegetation Chars across

672 Differing Burn Severity and Feedstock Types from Pacific Northwest, USA (V3),
673 <https://doi.org/10.15485/1894135>, 2022.

674 Gundale, M. J. and DeLuca, T. H.: Temperature and source material influence ecological
675 attributes of ponderosa pine and Douglas-fir charcoal, *For. Ecol. Manage.*, 231, 86–93, 2006.

676 Halofsky, J. E., Peterson, D. L., and Harvey, B. J.: Changing wildfire, changing forests: the
677 effects of climate change on fire regimes and vegetation in the Pacific Northwest, USA, *Fire
678 Ecology*, 16, 4, 2020.

679 Hatch, L. E., Jen, C. N., Kreisberg, N. M., Selimovic, V., Yokelson, R. J., Stamatis, C., York, R.
680 A., Foster, D., Stephens, S. L., Goldstein, A. H., and Barsanti, K. C.: Highly Speciated
681 Measurements of Terpenoids Emitted from Laboratory and Mixed-Conifer Forest Prescribed
682 Fires, *Environ. Sci. Technol.*, 53, 9418–9428, 2019.

683 Haugo, R. D., Kellogg, B. S., Cansler, C. A., Kolden, C. A., Kemp, K. B., Robertson, J. C.,
684 Metlen, K. L., Vaillant, N. M., and Restaino, C. M.: The missing fire: quantifying human
685 exclusion of wildfire in Pacific Northwest forests, USA, *Ecosphere*, 10, e02702, 2019.

686 Jolly, W. M., Cochrane, M. A., Freeborn, P. H., Holden, Z. A., Brown, T. J., Williamson, G. J.,
687 and Bowman, D. M. J. S.: Climate-induced variations in global wildfire danger from 1979 to
688 2013, *Nat. Commun.*, 6, 7537, 2015.

689 Keeley, J. E.: Fire intensity, fire severity and burn severity: a brief review and suggested usage,
690 *Int. J. Wildland Fire*, 18, 116–126, 2009.

691 Kelly, S. D., Hesterberg, D., and Ravel, B.: Analysis of soils and minerals using X-ray
692 absorption spectroscopy, in: *Methods of Soil Analysis Part 5—Mineralogical Methods*,
693 American Society of Agronomy and Soil Science Society of America, Madison, WI, USA, 387–
694 463, 2015.

695 Kruse, J., Abraham, M., Amelung, W., Baum, C., Bol, R., Kühn, O., Lewandowski, H.,
696 Niederberger, J., Oelmann, Y., Rüger, C., Santner, J., Siebers, M., Siebers, N., Spohn, M.,
697 Vestergren, J., Vogts, A., and Leinweber, P.: Innovative methods in soil phosphorus research: A
698 review, *J. Plant Nutr. Soil Sci.*, 178, 43–88, 2015.

699 Lane, P. N. J., Sheridan, G. J., Noske, P. J., and Sherwin, C. B.: Phosphorus and nitrogen exports
700 from SE Australian forests following wildfire, *J. Hydrol.*, 361, 186–198, 2008.

701 Lenth, R. V.: *emmeans: Estimated marginal means*, Github,
702 <https://doi.org/10.1080/00031305.1980.10483031>, 2023.

703 Li, B. and Brett, M. T.: The influence of dissolved phosphorus molecular form on recalcitrance
704 and bioavailability, *Environ. Pollut.*, 182, 37–44, 2013.

705 Lopez, A. M., Avila, C. C. E., VanderRoest, J. P., Roth, H. K., Fendorf, S., and Borch, T.:
706 Molecular insights and impacts of wildfire-induced soil chemical changes, *Nature Reviews Earth
707 & Environment*, 5, 431–446, 2024.

708 Makarov, M. I., Haumaier, L., Zech, W., Marfenina, O. E., and Lysak, L. V.: Can ³¹P NMR
709 spectroscopy be used to indicate the origins of soil organic phosphates?, *Soil Biol. Biochem.*, 37,
710 15–25, 2005.

711 McDowell, R. W., Worth, W., and Carrick, S.: Evidence for the leaching of dissolved organic
712 phosphorus to depth, *Sci. Total Environ.*, 755, 142392, 2021.

713 McMeeking, G. R., Kreidenweis, S. M., Baker, S., Carrico, C. M., Chow, J. C., Collett, J. L., Jr,
714 Hao, W. M., Holden, A. S., Kirchstetter, T. W., Malm, W. C., Moosmüller, H., Sullivan, A. P.,
715 and Wold, C. E.: Emissions of trace gases and aerosols during the open combustion of biomass
716 in the laboratory, *J. Geophys. Res. D: Atmos.*, 114, <https://doi.org/10.1029/2009JD011836>,
717 2009.

718 Merino, A., Jiménez, E., Fernández, C., Fontúrbel, M. T., Campo, J., and Vega, J. A.: Soil
719 organic matter and phosphorus dynamics after low intensity prescribed burning in forests and
720 shrubland, *J. Environ. Manage.*, 234, 214–225, 2019.

721 Mishra, A., Alnahit, A., and Campbell, B.: Impact of land uses, drought, flood, wildfire, and
722 cascading events on water quality and microbial communities: A review and analysis, *J. Hydrol.*,
723 596, 125707, 2021.

724 Mukherjee, A. and Zimmerman, A. R.: Organic carbon and nutrient release from a range of
725 laboratory-produced biochars and biochar–soil mixtures, *Geoderma*, 193–194, 122–130, 2013.

726 Myers-Pigg, A. N., Grieger, S., Roebuck, J. A., Jr, Barnes, M. E., Bladon, K. D., Bailey, J. D.,
727 Barton, R., Chu, R. K., Graham, E. B., Homolka, K. K., Kew, W., Lipton, A. S., Scheibe, T.,
728 Toyoda, J. G., and Wagner, S.: Experimental Open Air Burning of Vegetation Enhances Organic
729 Matter Chemical Heterogeneity Compared to Laboratory Burns, *Environ. Sci. Technol.*, 58,
730 9679–9688, 2024.

731 Noack, S. R., McLaughlin, M. J., Smernik, R. J., McBeath, T. M., and Armstrong, R. D.: Crop
732 residue phosphorus: speciation and potential bio-availability, *Plant Soil*, 359, 375–385, 2012.

733 Parsons, A., Robichaud, P., Lewis, S. A., Napper, C., and Clark, J. T.: Field guide for mapping
734 post-fire soil burn severity, United States Department of Agriculture Forest Service Rocky
735 Mountain Research Station, <https://doi.org/10.2737/RMRS-GTR-243>, 2010.

736 R Core Team: *R: A Language and Environment for Statistical Computing*, 2023.

737 Randerson, J. T., Chen, Y., van der Werf, G. R., Rogers, B. M., and Morton, D. C.: Global
738 burned area and biomass burning emissions from small fires, *Biogeosciences*, 117,
739 <https://doi.org/10.1029/2012JG002128>, 2012.

740 Ravel, B. and Newville, M.: ATHENA, ARTEMIS, HEPHAESTUS: data analysis for X-ray
741 absorption spectroscopy using IFEFFIT, *J. Synchrotron Radiat.*, 12, 537–541, 2005.

742 Recena, R., Cade-Menun, B. J., and Delgado, A.: Organic phosphorus forms in agricultural soils
743 under Mediterranean climate, *Soil Sci. Soc. Am. J.*, 82, 783–795, 2018.

744 Reilly, M. J., Dunn, C. J., Meigs, G. W., Spies, T. A., Kennedy, R. E., Bailey, J. D., and Briggs,
745 K.: Contemporary patterns of fire extent and severity in forests of the Pacific Northwest, USA
746 (1985–2010), *Ecosphere*, 8, e01695, 2017.

747 Robinson, J. S., Baumann, K., Hu, Y., Hagemann, P., Kebelmann, L., and Leinweber, P.:
748 Phosphorus transformations in plant-based and bio-waste materials induced by pyrolysis, *Ambio*,
749 47, 73–82, 2018.

750 Roebuck, J. A., Jr, Grieger, S., Barnes, M. E., Gillespie, X., Bladon, K. D., Bailey, J. D.,
751 Graham, E. B., Chu, R., Kew, W., Scheibe, T. D., and Myers-Pigg, A. N.: Molecular shifts in
752 dissolved organic matter along a burn severity continuum for common land cover types in the
753 Pacific Northwest, USA, *Sci. Total Environ.*, 958, 178040, 2024.

754 Rose, T. J., Schefe, C., Weng, Z. (han), Rose, M. T., van Zwieten, L., Liu, L., and Rose, A. L.:
755 Phosphorus speciation and bioavailability in diverse biochars, *Plant Soil*, 443, 233–244, 2019.

756 Rust, A. J., Hogue, T. S., Saxe, S., and McCray, J.: Post-fire water-quality response in the
757 western United States, *Int. J. Wildland Fire*, 27, <https://doi.org/10.1071/WF17115>, 2018.

758 Saa, A., Trasar-Cepeda, M. C., Gil-Sotres, F., and Carballas, T.: Changes in soil phosphorus and
759 acid phosphatase activity immediately following forest fires, *Soil Biol. Biochem.*, 25, 1223–
760 1230, 1993.

761 Santín, C., Doerr, S. H., Merino, A., Bucheli, T. D., Bryant, R., Ascough, P., Gao, X., and
762 Masiello, C. A.: Carbon sequestration potential and physicochemical properties differ between
763 wildfire charcoals and slow-pyrolysis biochars, *Sci. Rep.*, 7, 11233, 2017.

764 Santín, C., Otero, X. L., Doerr, S. H., and Chafer, C. J.: Impact of a moderate/high-severity
765 prescribed eucalypt forest fire on soil phosphorous stocks and partitioning, *Sci. Total Environ.*,
766 621, 1103–1114, 2018.

767 Schaller, J., Tischer, A., Struyf, E., Bremer, M., Belmonte, D. U., and Potthast, K.: Fire enhances
768 phosphorus availability in topsoils depending on binding properties, *Ecology*, 96, 1598–1606,
769 2015.

770 Silber, A., Levkovitch, I., and Graber, E. R.: pH-dependent mineral release and surface
771 properties of cornstraw biochar: agronomic implications, *Environ. Sci. Technol.*, 44, 9318–9323,
772 2010.

773 Silins, U., Bladon, K. D., Kelly, E. N., Esch, E., Spence, J. R., Stone, M., Emelko, M. B., Boon,
774 S., Wagner, M. J., Williams, C. H. S., and Tichkowsky, I.: Five-year legacy of wildfire and
775 salvage logging impacts on nutrient runoff and aquatic plant, invertebrate, and fish productivity,
776 *Ecohydrol.*, 7, 1508–1523, 2014.

777 Smil, V.: PHOSPHORUS IN THE ENVIRONMENT: Natural Flows and Human Interferences,
778 *Annu. Rev. Environ. Resour.*, 25, 53–88, 2000.

779 Son, J.-H., Kim, S., and Carlson, K. H.: Effects of Wildfire on River Water Quality and Riverbed
780 Sediment Phosphorus, *Water Air Soil Pollut. Focus*, 226, 26, 2015.

781 Souza-Alonso, P., Prats, S. A., Merino, A., Guiomar, N., Guijarro, M., and Madrigal, J.: Fire
782 enhances changes in phosphorus (P) dynamics determining potential post-fire soil recovery in
783 Mediterranean woodlands, *Sci. Rep.*, 14, 21718, 2024.

784 Stavi, I.: Wildfires in Grasslands and Shrublands: A Review of Impacts on Vegetation, Soil,
785 Hydrology, and Geomorphology, *Water*, 11, 1042, 2019.

786 Sun, K., Qiu, M., Han, L., Jin, J., Wang, Z., Pan, Z., and Xing, B.: Speciation of phosphorus in
787 plant- and manure-derived biochars and its dissolution under various aqueous conditions, *Sci.*
788 *Total Environ.*, 634, 1300–1307, 2018.

789 Turner, B. L., Cade-Menun, B. J., and Westermann, D. T.: Organic Phosphorus Composition and
790 Potential Bioavailability in Semi-Arid Arable Soils of the Western United States, Published in
791 *Soil Sci. Soc. Am. J.*, 67, 1168–1179, 2003a.

792 Turner, B. L., Mahieu, N., and Condon, L. M.: Phosphorus-31 nuclear magnetic resonance
793 spectral assignments of phosphorus compounds in soil NaOH–EDTA extracts, *Soil Sci. Soc.*
794 *Am. J.*, 67, 497–510, 2003b.

795 Turrion, M.-B., Lafuente, F., Aroca, M.-J., López, O., Mulas, R., and Ruipérez, C.:
796 Characterization of soil phosphorus in a fire-affected forest Cambisol by chemical extractions
797 and 31P-NMR spectroscopy analysis, *Sci. Total Environ.*, 408, 3342–3348, 2010.

798 Uchimiya, M. and Hiradate, S.: Pyrolysis temperature-dependent changes in dissolved
799 phosphorus speciation of plant and manure biochars, *J. Agric. Food Chem.*, 62, 1802–1809,
800 2014.

801 Uchimiya, M., Hiradate, S., and Antal, M. J., Jr: Dissolved Phosphorus Speciation of Flash
802 Carbonization, Slow Pyrolysis, and Fast Pyrolysis Biochars, *ACS Sustainable Chem. Eng.*, 3,
803 1642–1649, 2015.

804 Method 365.3: Phosphorus, All Forms (Colorimetric, Ascorbic Acid, Two Reagent):
805 https://www.epa.gov/sites/default/files/2015-08/documents/method_365-3_1978.pdf.

806 Vega, J. A., Fontúrbel, T., Merino, A., Fernández, C., Ferreira, A., and Jiménez, E.: Testing the
807 ability of visual indicators of soil burn severity to reflect changes in soil chemical and microbial
808 properties in pine forests and shrubland, *Plant Soil*, 369, 73–91, 2013.

809 Weihrauch, C. and Opp, C.: Ecologically relevant phosphorus pools in soils and their dynamics:
810 The story so far, *Geoderma*, 325, 183–194, 2018.

811 Werner, F. and Prietzel, J.: Standard Protocol and Quality Assessment of Soil Phosphorus
812 Speciation by P K-Edge XANES Spectroscopy, *Environ. Sci. Technol.*, 49, 10521–10528, 2015.

813 Wu, H., Yip, K., Kong, Z., Li, C.-Z., Liu, D., Yu, Y., and Gao, X.: Removal and Recycling of
 814 Inherent Inorganic Nutrient Species in Mallee Biomass and Derived Biochars by Water
 815 Leaching, *Ind. Eng. Chem. Res.*, 50, 12143–12151, 2011.

816 Wu, Y., Pae, L. M., Gu, C., and Huang, R.: Phosphorus Chemistry in Plant Ash: Examining the
 817 Variation across Plant Species and Compartments, *ACS Earth Space Chem.*,
 818 <https://doi.org/10.1021/acsearthspacechem.3c00145>, 2023a.

819 Wu, Y., Pae, L. M., and Huang, R.: Phosphorus chemistry in plant charcoal: interplay between
 820 biomass composition and thermal condition, *Int. J. Wildland Fire*, 33, NULL-NULL, 2023b.

821 Xu, G., Zhang, Y., Shao, H., and Sun, J.: Pyrolysis temperature affects phosphorus
 822 transformation in biochar: Chemical fractionation and 31P NMR analysis, *Sci. Total Environ.*,
 823 569–570, 65–72, 2016.

824 Yan, Y., Wan, B., Jiang, R., Wang, X., Wang, H., Lan, S., Zhang, Q., and Feng, X.: Interactions
 825 of organic phosphorus with soil minerals and the associated environmental impacts: A review,
 826 *Pedosphere*, 33, 74–92, 2023.

827 Yu, F., Wang, J., Wang, X., Wang, Y., Guo, Q., Wang, Z., Cui, X., Hu, Y., Yan, B., and Chen,
 828 G.: Phosphorus-enriched biochar from biogas residue of *Eichhornia crassipes*: transformation
 829 and release of phosphorus, *Biochar*, 5, 82, 2023.

830 Yusiharni, E. and Gilkes, R.: Minerals in the ash of Australian native plants, *Geoderma*, 189–
 831 190, 369–380, 2012.

832 Zavala, L. M., De Celis, R., and Jordán, A.: How wildfires affect soil properties. A brief review,
 833 *Cuad. Investig. Geogr.*, 40, 311–332, 2014.

834 Zheng, H., Wang, Z., Deng, X., Zhao, J., Luo, Y., Novak, J., Herbert, S., and Xing, B.:
 835 Characteristics and nutrient values of biochars produced from giant reed at different
 836 temperatures, *Bioresour. Technol.*, 130, 463–471, 2013.

837 Zwetsloot, M. J., Lehmann, J., and Solomon, D.: Recycling slaughterhouse waste into fertilizer:
 838 how do pyrolysis temperature and biomass additions affect phosphorus availability and
 839 chemistry?, *J. Sci. Food Agric.*, 95, 281–288, 2015.